Unraveling Proteins: A Molecular Mechanics Study

Remo Rohs, Catherine Etchebest, and Richard Lavery
Laboratoire de Biochimie Théorique, Institut de Biologie Physico-Chimique, Paris 75005, France

ABSTRACT An internal coordinate molecular mechanics study of unfolding peptide chains by external stretching has been carried out to predict the type of force spectra that may be expected from single-molecule manipulation experiments currently being prepared. Rather than modeling the stretching of a given protein, we have looked at the behavior of simple secondary structure elements (α-helix, β-ribbon, and interacting α-helices) to estimate the magnitude of the forces involved in their unfolding or separation and the dependence of these forces on the way pulling is carried out as well as on the length of the structural elements. The results point to a hierarchy of forces covering a surprisingly large range and to important orientational effects in the response to external stress.

INTRODUCTION

Over the last few years, very fruitful collaborations between physicists, chemists, and biologists have led to the possibility of trapping and manipulating individual biological macromolecules (Bensimon, 1996; Austin et al., 1997). This is a very exciting development as it offers direct access to the mechanical properties of molecules and molecular complexes, under controlled physico-chemical conditions, and without the usual statistical filter that separates experiments on bulk material from the underlying molecular behavior.

Single-molecule experiments have already been carried out on nucleic acids (Cluzel et al., 1996; Smith et al., 1996; Strick et al., 1996, 1998; Allemand et al., 1998; Essevaz-Roulet et al., 1997; Bockelmann et al., 1997; Lee et al., 1994a; Noy et al., 1997), proteins (Tskhovrebova et al., 1997; Rief et al., 1997a; Kellermayer et al., 1997), protein-protein complexes (Florin et al. 1994; Lee et al., 1994b), protein-DNA complexes (Yin et al., 1995), and polysaccharides (Rief et al., 1997b). Duplex DNA has notably been the subject of many experiments that have tested the response of polymeric molecules to stretching (Cluzel et al., 1996; Smith et al., 1996), twisting (Strick et al., 1996, 1998; Allemand et al., 1998), and strand separation (Essevaz-Roulet et al., 1997; Bockelmann et al., 1997), whereas other experiments have studied the stretching of short oligomers (Lee et al., 1994; Noy et al., 1997). The external constraints on the molecules in question have been imposed with a variety of techniques, including micropipettes, laser traps, magnets acting on paramagnetic microbeads, or the cantilevers of atomic force microscopes. In each case, it has been possible to measure the forces involved in deforming the molecules and in destroying their intra- or intermolecular interactions as a result of pulling, twisting, or shearing movements.

The forces related to such deformations typically range from several piconewtons (pN) for overcoming the entropic resistance of randomly coiled polymers, to roughly 100 pN for inducing large molecular deformations, and finally into the range of tens of nanonewtons (nN) for breaking chemical bonds. (It is useful to note that a change in energy of 1 kcal/mol/Å corresponds to a force of roughly 70 pN).

Going beyond a knowledge of the forces derived from these nanomanipulation experiments requires a contribution from molecular simulations. Both molecular mechanics and molecular dynamics have already been used in relating forces to structural and energetic changes. In the case of the first experiments on antibody-antigen interactions (streptavidin-biotin), the simulations carried out by Grubmüller et al. (1996) and by the group of Schulten (Izrailev et al., 1997) led to a deeper understanding of the detailed events involved in separating this archetypal intermolecular complex. In the case of DNA, modeling has brought to light new forms of the double helix that result from extreme stretching (Cluzel et al., 1996; Konrad and Bolonick, 1996; Lebrun and Lavery, 1996, 1998) and have subsequently turned out to occur locally at sites where certain minor groove binding proteins interact with the double helix (Lebrun et al., 1997). Other studies in this field have shown that the positive supercoiling of DNA molecules held under tension can also lead to the formation a very surprising conformation with tightly interwound phosphodiester backbones and exposed bases (Allemand et al., 1998).

Recently, major structural deformations have also been created within a protein. Using the giant muscle fiber protein titin, three groups of investigators (Tskhovrebova et al., 1997; Rief et al., 1997a; Kellermayer et al., 1997) have observed elastic behavior that indicates that beyond a certain limiting force (variously measured as falling between 20 and 250 pN) a hysteresis occurs in the stretching-relaxation force curve that has been attributed to the denaturation (and the subsequent, slow renaturation) of the immunoglobulin-like domains that occur in regular repeats along the titin

Received for publication 7 October 1998 and in final form 3 February 1999.

Address reprint requests to Dr. Richard Lavery, Institut de Biologie Physico-Chimique, 13 rue Pierre et Marie Curie, Paris 75005, France. Tel.: 33-1-43252609; Fax: 33-1-43295645; E-mail: richard@ibpc.fr.

R. Rohs' permanent address: Theoretical Biophysics Group, Max Delbrück Institute of Molecular Medicine, Robert Rössle Strasse 10, Berlin Buch, Germany.

0006-3495/99/05/2760/09 $2.00

polypeptide chain. This result indicates that it may be possible to obtain very interesting information on protein denaturation mechanisms in this way and, hopefully, to relate such information to the biologically and biotechnologically vital question of protein folding. Consequently, a number of groups are now preparing experiments that will allow the mechanical properties of single globular proteins to be studied, most probably via the construction of manipulable chimeric species having DNA strings attached to the protein termini.

Understanding the behavior of such constructs is an important challenge for molecular simulation as it will determine in large part how much structural information we will be able to extract from the measured forces. Such simulations will also contribute to analyzing future studies on protein-nucleic acid complexes, which represent another field of considerable biological interest.

Although the mechanics of the DNA double helix under stress now begins to be understood, very little is known about the mechanics of globular proteins. We have consequently decided to begin our investigations by calculating the forces involved in deforming the secondary structures from which globular proteins are built, rather than by directly studying a complete protein molecule. In this way, we hope to be able to predict the manner in which a protein will come apart under mechanical stress and thus to be able to interpret the force spectra that will undoubtedly be available via single-molecule manipulation experiments.

We have also chosen to perform these studies using molecular mechanics and, more specifically, adiabatic mapping as a function of imposed distance constraints. This approach enables us to use a simplified internal coordinate representation of the oligopeptides, which reduces the number of variables to be taken into account and diminishes problems related to local energy minima. We also employ a simplified continuum solvent representation. A similar technique has already been used to good effect for studying DNA deformation and has led to results in accord with experiment (Cluzel et al., 1996; Allemand et al., 1998; Lebrun and Lavery, 1996, 1998). Although molecular dynamics simulations could also be used for such numerical experiments (Grubmüller et al., 1996; Izrailev et al., 1997; Konrad and Bolonick, 1996), and are indeed necessary to study thermal fluctuation effects, this approach has the disadvantage of being computationally much more expensive, limiting the number of molecular structures that can be studied. In the case of explicitly applied forces, it also should to be noted that the use of nanosecond scale trajectories implies provoking molecular deformations many orders of magnitude faster than in the laboratory experiments, which strongly influences the resulting forces (Evans and Ritchie, 1997).

METHODS

The present simulations have been carried out with the program LIGAND, which is closely related to the JUMNA program used for modeling nucleic acids (Lavery et al., 1995). However, in contrast to the latter program, which uses a combination of helical and internal coordinates, LIGAND functions entirely in internal coordinates. In the case of polypeptides, all bond lengths and valence angles are frozen (with the exception of the intracyclic angles of the flexible proline ring). The FLEX force field, whose formulation is given below, includes nonbonded electrostatic and Lennard-Jones terms (*nb*), torsion (ϕ), and valence angle (θ) terms as well as length restraints (l) for proline ring closure or corresponding to external length constraints. Hydrogen bonding is treated using a special Lennard-Jones term (*HB*), which reproduces the angular dependence of such interactions (where θ_{HB} is the angle formed by the vectors D-H and H. . . A of a bond D-H. . . A). FLEX parameterization, including the calculation of point charges appropriate for polypeptides, has been described elsewhere (Lavery et al., 1995, 1986; Zakrzewska et al., 1985)

$$E = \sum_{nb}\left(\frac{q_i q_j}{\epsilon r_{ij}} + \frac{A_{ij}}{r_{ij}^{12}} - \frac{B_{ij}}{r_{ij}^{6}}\right) + \sum_{\phi}\frac{V_\phi}{2}[1 + \mathrm{Cos}(n\phi - \gamma)] + \sum_{\theta} K_\theta(\theta - \theta_{eq})^2 + \sum_{l} K_l(l - l_{eq})^2 + \sum_{HB}\mathrm{Cos}\theta_{HB}\left[\left(\frac{A_{ij}^{HB} - A_{ij}}{r_{ij}^{12}}\right) - \left(\frac{B_{ij}^{HB} - B_{ij}}{r_{ij}^{6}}\right)\right]$$

To conserve the advantage of an internal coordinate approach, it is necessary to represent solvent and counterion effects with a continuum model. We presently do this using a sigmoidal distance-dependent dielectric function (Lavery et al., 1995; Hingerty et al., 1985), with adjustable slope (S) and plateau (D) values. The formula used for the dielectric damping is shown below:

$$\epsilon(r) = D - \frac{(D - D_0)}{2}[(rS)^2 + 2rS + 2]\exp(-rS)$$

Following the work of Ahora and Jayaram (1997) we have introduced an additional parameter, D_0, which enables the value of $\epsilon(r)$ at $r = 0$ to be adjusted. This parameter has a notable effect on the strength of hydrogen bonding. Using conventional distance-dependent dielectric damping (with either sigmoidal or linear forms) generally leads to reinforced hydrogen bonding, even though intermediate and long-range charge-charge interactions are strongly damped. This occurs because the electrostatic component of hydrogen bonds is basically dipolar in nature, D($\delta-$)-H($\delta+$). . . A($\delta-$), and the distance-dependent damping shields the longer-range, repulsive interactions between the donor (D) and acceptor atoms (A) more than the short-range, attractive interactions between the hydrogen atom and the acceptor. Setting D_0 greater than zero both increases damping and decreases the slope of $\epsilon(r)$ in the range where hydrogen bonding occurs. We have presently used values of $D_0 = 4$, $D = 80$, and $S = 0.4$. With this set of parameters a single hydrogen bond within a canonical α-helix has an energy of 1.8 kcal/mol, which is slightly above the value estimated for an isolated peptide hydrogen bond in water (~1–1.5 kcal/mol) (Ahora and Jayaram, 1997 and references therein) and well below the vacuum value of 4.8 kcal/mol obtained with our parameterization. This value should be appropriate for modeling a hydrogen bond in a denaturing protein, where, even if the bond occurs close to the solvent interface, it is still partially shielded from the solvent environment.

To simplify the architectural elements we study as much as possible, we have presently used only oligoalanine fragments (with the single exception of a proline residue within an α-helix). This avoids any problems related to optimizing the conformations of close-packed side chains but is clearly a simplification that needs to be removed in the future (see conclusions). Secondary structural motifs were built using standard geometries (right-handed α-helix: ϕ −57/ψ −47; anti-parallel β ribbon: ϕ −139/ψ 135) and then energy minimized. All oligopeptides had neutral HCO and NH_2 terminal groups.

Deformations were carried out using adiabatic mapping as a function of a single distance constraint. Each mapping consisted of imposing a chosen distance between a chosen pair of atoms, performing an energy minimization, making a slight increase in the constraint distance, reminimizing, and then repeating this procedure until the desired distance had been reached (Cluzel et al., 1996; Lebrun and Lavery, 1996, 1998). Using steps varying between 0.1 and 0.25 Å depending on the deformation studied, this procedure typically required of the order of 200–400 minimizations for each one-dimensional map. Forces were derived by the analytic differentiation of polynomial functions fitted to the corresponding energy curves, using a sixth-order polynomial and a single-value decomposition algorithm (Press et al., 1992).

RESULTS

We present below the mechanical properties of the principal architectural elements found in globular proteins when subjected to external stretching. We have treated the α-helix, anti-parallel β-ribbons, and two anti-parallel interacting α-helices. The various deformations that have been studied using adiabatic energy mapping are shown schematically in Fig. 1.

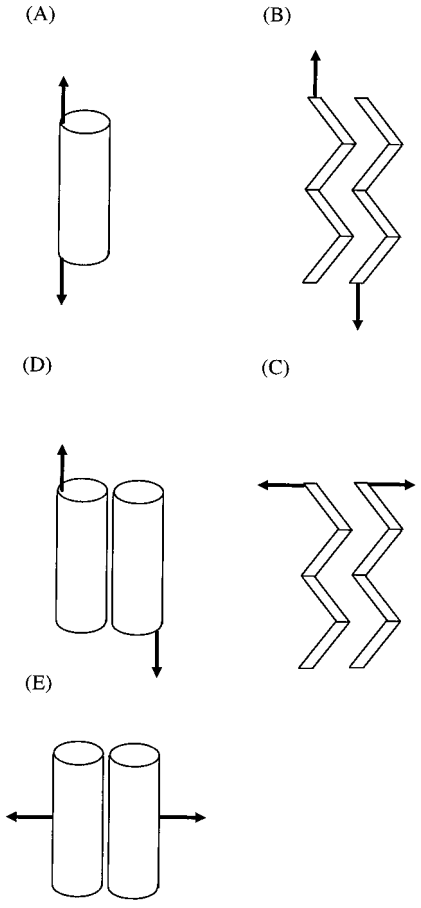

FIGURE 1 Schematic diagrams of the various deformations studied. α-Helices are symbolized as cylinders and β-strands as folded strips. Both β-ribbons and α-helix pairs were anti-parallel. The arrows indicate the positions where the stretching constraints were applied and the direction of stretching. The letters indicate the corresponding results sections.

(A) α-Helix stretching

A canonical right-handed α-helix was built using an oligopeptide composed of 20 alanine residues. After energy minimization, a distance constraint was applied between the first and last Cα atoms (initial value, 28.6 Å), and the helix was stretched by increasing this distance by intervals of 0.1 Å, reminimizing the conformation at each step. The solid line in Fig. 2 *A* shows the energy variation as a function of stretching. This curve increases rather smoothly up to a relative length of almost 2.0 (i.e., measured with respect to the length of the relaxed helix). This stretching, which occurs rather uniformly along the molecule, actually involves two distinct conformational transitions that provoke the conversion of the α-helix into a 3_{10}-helix and then into an extended form approaching the β-ribbon conformation. These transitions can be followed by counting the hydrogen bonds within the molecule. Fig. 2 *B* shows that, as stretching progress, the 1–4 hydrogen bonds of the α-helix (solid line) are smoothly replaced by the 1–3 hydrogen bonds of the 3_{10}-helix (dotted line). Once this transition is completed, the 3_{10}-helix hydrogen bonds start to break and the structure further extends toward the β-ribbon conformation. These changes can be followed graphically in Fig. 3.

It is possible to obtain the forces corresponding to these transitions by differentiating a polynomial fitted to the energy curve. The resulting force variation (Fig. 2 *C*, solid line) shows a slow initial rise as the helix undergoes elastic deformation. This is followed by an inflection in the curve as the structural transitions begin, recalling the force plateau seen when stretching double-helical DNA molecules (Cluzel et al., 1996; Lebrun and Lavery, 1996, 1998). However, the forces involved (~500 pN) here are almost seven times higher than those measured for DNA.

In fact, the more or less uniform extension of the α-helix is not an energetically optimal solution as shown by the dashed curve in Fig. 2 *A*. This alternative pathway consists of unwinding the α-helix turn by turn rather than uniformly and extending each turn fully to a β-ribbon conformation (see Fig. 4). (The results shown correspond to the successive unwinding of two turns of the α-helix.) Although, this pathway involves a steeper energy rise for small extensions and thus considerably higher forces (see dashed line in Fig. 2 *C*), it rapidly becomes energetically preferable.

We have made a very preliminary study of sequence effects on α-helix stretching by introducing a single proline residue into the alanine oligopeptide. The absence of an amide hydrogen and the restricted values of ϕ associated with the proline ring cause the loss of an (i)–$(i + 4)$ hydrogen bond within the helix and commonly induce helix kinking. As can be seen in Fig. 2 *A*, the presence of a single proline (placed at the center of the helix) produces only a slight weakening of the structure as seen in the force curve given in Fig. 2 *C* (dotted line). This effect becomes more important for larger extensions, but, as discussed above, the uniform stretching pathway is not optimal in this region. It is remarked that the forces, shown in Fig. 2 *C*, can be

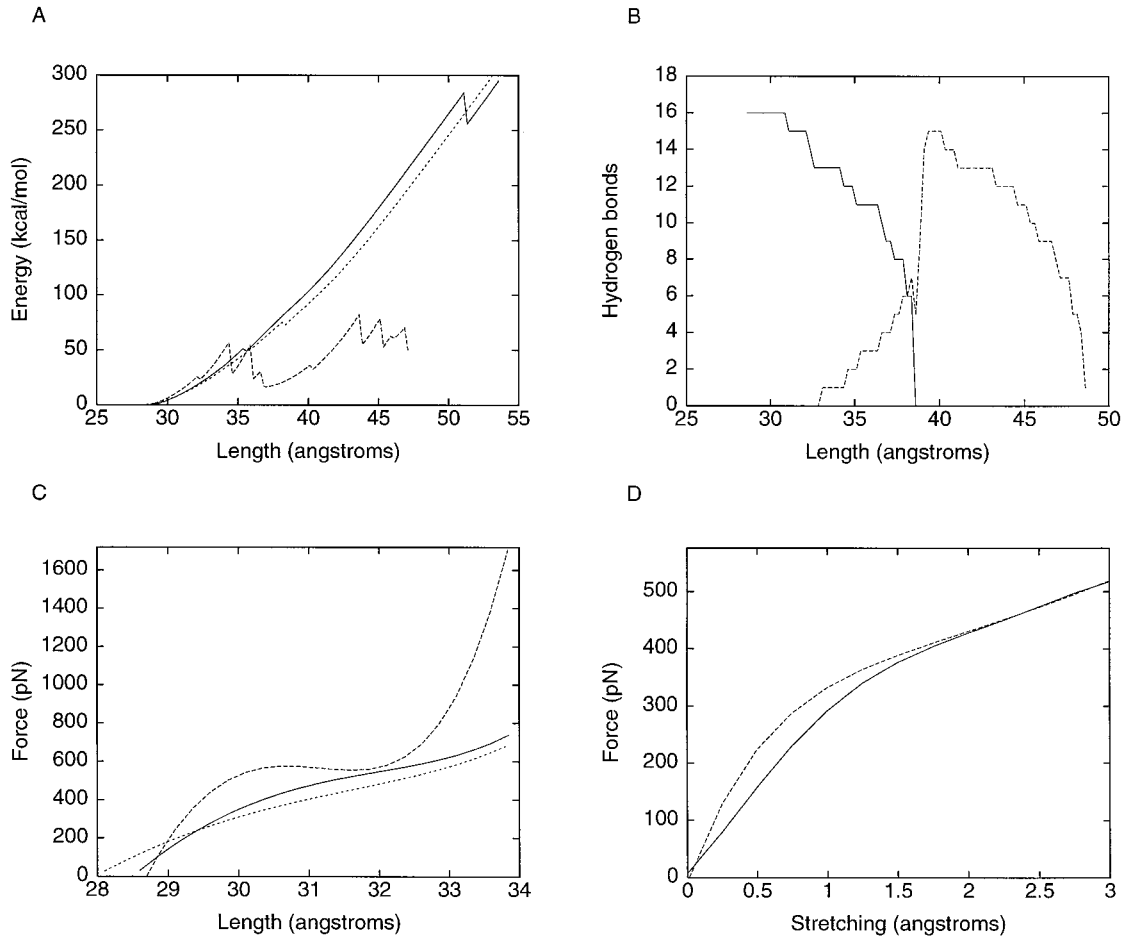

FIGURE 2 α-Helix stretching. (*A*) Conformational energy as a function of length. (*B*) Total number of hydrogen bonds. (*C*) Force curve. (*D*) Length effect on force curve. In *A* and *C*: ——, uniform stretching of an $(Ala)_{20}$ α-helix; · · ·, uniform stretching of an $(Ala)_9$-Pro-$(Ala)_{10}$ α-helix; - - -, turn-by-turn stretching of $(Ala)_{20}$. In *B*: ——, (i)–$(i + 4)$ hydrogen bonds; - - -, (i)–$(i + 3)$ hydrogen bonds. In *D*: ——, $(Ala)_{20}$; - - -, $(Ala)_{12}$.

calculated only for the relatively smooth section at the beginning of the stretching curves. However, in the case of the turn-by-turn pathway it is also found that very similar forces are necessary for destroying successive turns of the helix.

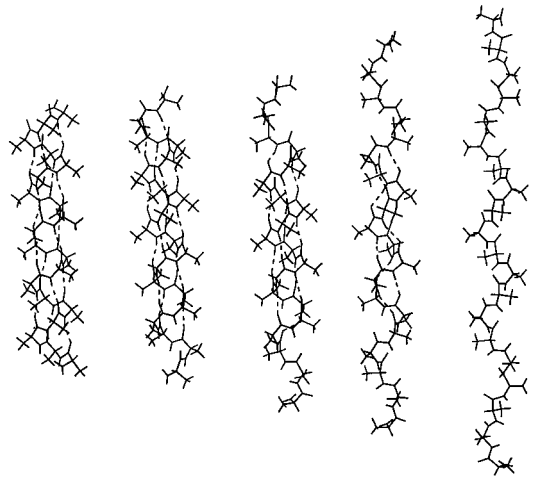

FIGURE 3 Snapshots of uniform α-helix stretching for the $(Ala)_{20}$ oligopeptide.

We can lastly consider length effects on α-helix stretching. For the energetically favorable turn-by-turn unwinding pathway, no length effects are to be expected as the conformational transition occurs locally one turn at a time. In fact, even the uniform extension pathway leads to forces that are almost independent of length. This is shown in Fig. 2 *D*, which compares the force curves obtained with α-helices having 20 (solid line) and 12 (dashed line) residues for a common extension of 3 Å.

(B) β-Ribbon: longitudinal shearing

We carried out longitudinal shearing on an anti-parallel β-ribbon formed of two $(Ala)_{10}$ oligopeptide chains. The chains were pulled apart longitudinally using a distance constraint between the two carboxyl-terminal Cα atoms. The resulting energy curve is shown in Fig. 5 *A*, and the evolving conformation is shown graphically in Fig. 6. The energy curve is quite unlike that of the α-helix (Fig. 2 *A*) and shows an alternation of sharp energy barriers followed

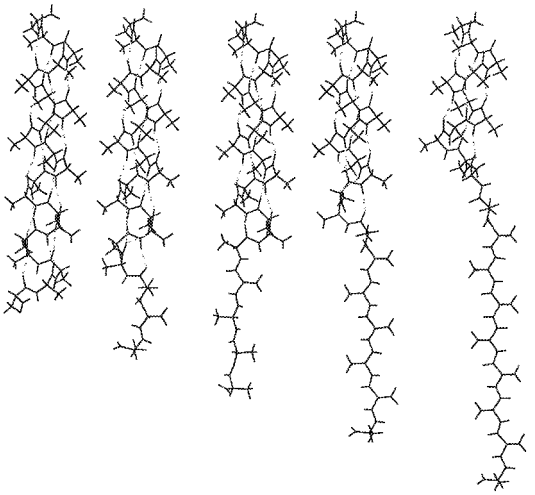

FIGURE 4 Snapshots of turn-by-turn α-helix stretching for the $(Ala)_{20}$ oligopeptide.

by flat wells. This behavior is linked to the fact that all of the hydrogen bonds that link the two β-strands lie perpendicularly to the shearing direction. Consequently, as stretching progresses, these bonds are first distorted laterally, for little energy cost, and then completely lost, almost concurrently, before being reformed after a shift in the alignment by two peptide groups (see Fig. 6). This means that the total number of hydrogen bonds decreases by two after each slippage, as shown clearly in Fig. 5 *B*. It can also be noted that, as the peptide backbones within the β-ribbon are almost fully extended, they undergo little deformation during the shearing process.

The principle forces associated with this stretching pathway occur as the hydrogen bonds linking the two strands are ruptured. They can be calculated from the sharp upward slopes preceding the energy wells in Fig. 5 *A*. For the first such barrier, the shearing force exceeds 1.5 nN, but this value drops more or less linearly as the number of hydrogen bonds decreases, and for the third peak, corresponding to six remaining hydrogen bonds, the force reaches a plateau value of roughly 700 pN (see Fig. 5 *C*).

(C) β-Ribbon: lateral shearing

We induced strand separation in an anti-parallel β-ribbon using a distance constraint between the two terminal Cα atoms at one end of the ribbon. Each strand was again formed by an $(Ala)_{10}$ oligopeptide. The energy variation as a function of stretching is shown in Fig. 7, and snapshots of the evolving pathway are given in Fig. 8. In this case, in contrast to the longitudinal shearing described above, the energy variation is roughly monotonic as shearing takes place. This is explained by a successive rather than a concurrent rupture of the hydrogen bonds joining the strands. If we derive the corresponding forces, again via a polynomial fit to the energy curve, we find an average around 40 pN with peaks of up to 120 pN. Once again, shearing is largely

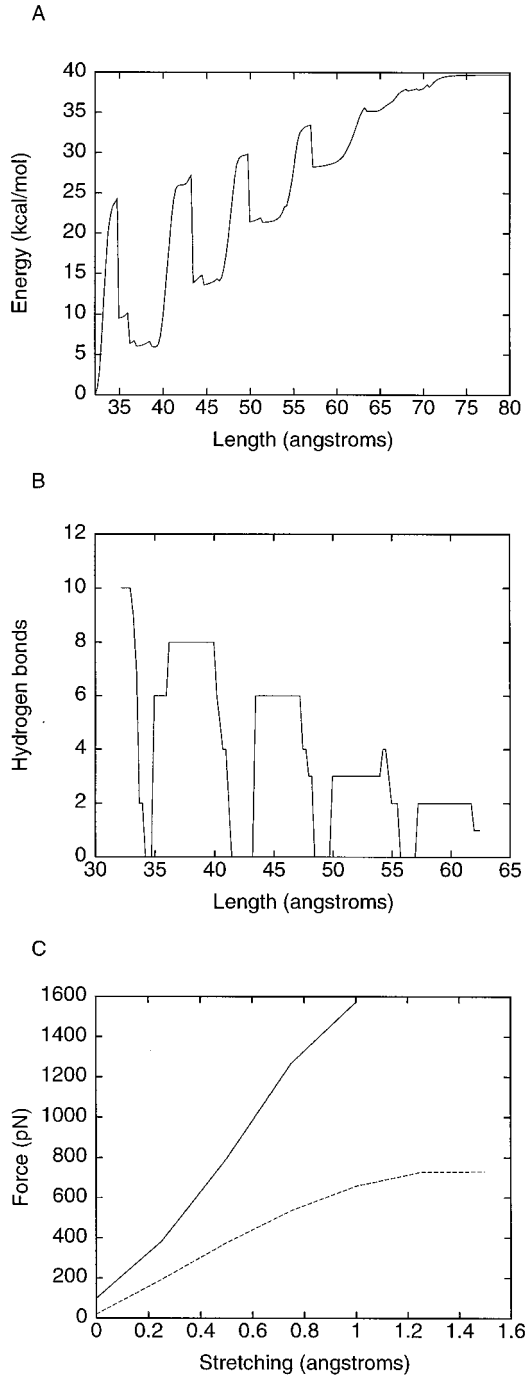

FIGURE 5 β-Ribbon longitudinal shearing. (*A*) Conformational energy as a function of length. (*B*) Total number of hydrogen bonds. (*C*) Force curve (——, forces corresponding to the first energy peak in energy plot; - - -, forces corresponding to the third peak in the energy plot).

limited to breaking hydrogen bonds as, with the exception of kinks at the strand separation point, there is little conformational change in the extended peptide backbones.

(D) Interacting α-helices: longitudinal shearing

We have carried out longitudinal shearing using two $(Ala)_{12}$, close-packed, anti-parallel α-helices using a dis-

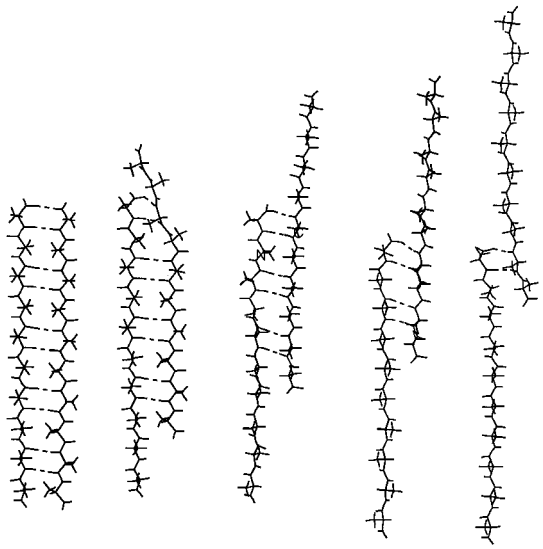

FIGURE 6 Snapshots of β-ribbon longitudinal shearing for two $(Ala)_{10}$ oligopeptides.

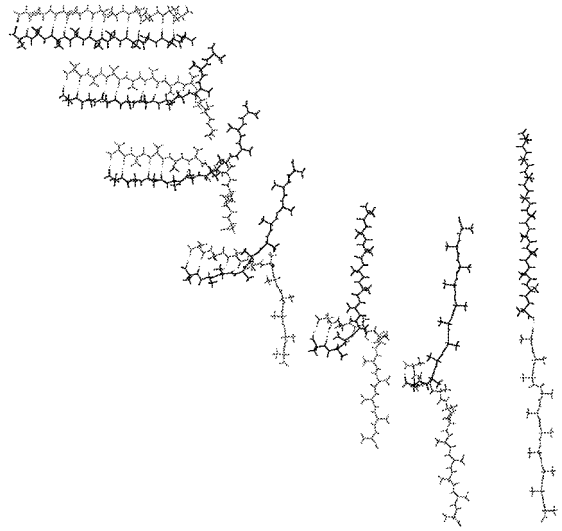

FIGURE 8 Snapshots of β-ribbon lateral shearing for two $(Ala)_{10}$ oligopeptides.

tance constraint between their carboxyl-terminal Cα atoms. The resulting energy curve (Fig. 9) shows a series of rather sharp peaks as the alanine side chains slide over one another and the total overlap area between the helices decreases. Fig. 10 illustrates the corresponding conformations. The average slope of the energy curve (18 kcal/mol lost over roughly 20 Å) corresponds to a force of roughly 65 pN, but the energy peaks lead to forces reaching roughly 150 pN, which, as can be judged from Fig. 9, are not very dependent on the extent to which the helices have already been separated.

(E) Interacting α-helices: lateral shearing

Lateral shearing was again carried with two $(Ala)_{12}$ antiparallel helices, initially in a close-packed conformation. Separation was performed by increasing the distance between the central Cα atoms of each helix, keeping the helical axes perpendicular to the separation direction. Note that although the initial value of the constrained distance was 11 Å, the actual separation between the helix axes in the relaxed dimer was 7.5 Å. The energy curve for lateral shearing is shown in Fig. 11. As might be expected, this profile is much smoother than for longitudinal movement, and it reaches a stable plateau after 5 Å of movement. The mean force for this action (~200 pN) is, however, rather strong. A test of the length dependence of lateral shearing indicates that passing from 12 to 20 residue helices (four to five α-helical turns) increases the separation force to roughly 350 pN (data not shown).

DISCUSSION

We have looked at how five typical structures found within globular proteins can be destroyed by external constraints. The results of adiabatic mapping using an internal coordinate model are summarized in Table 1. These data show a wide range of responses linked both to the architecture of

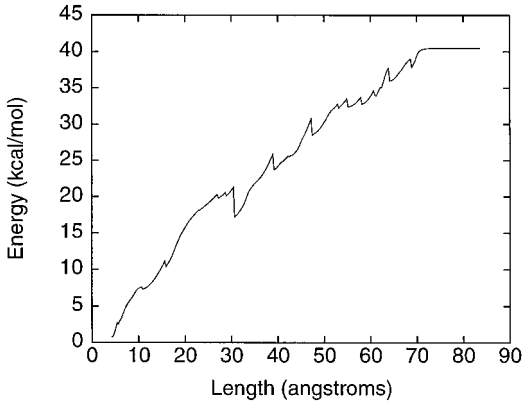

FIGURE 7 β-Ribbon lateral shearing: conformational energy as a function of length.

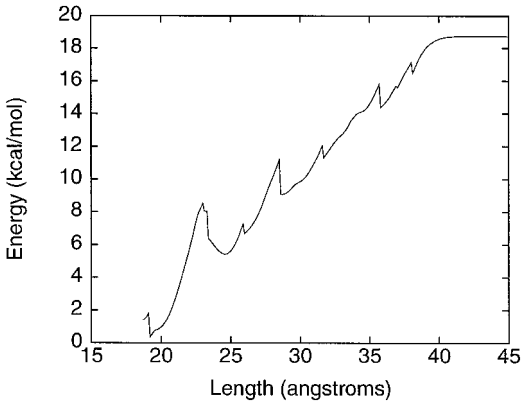

FIGURE 9 α-Helix longitudinal shearing: conformational energy as a function of length.

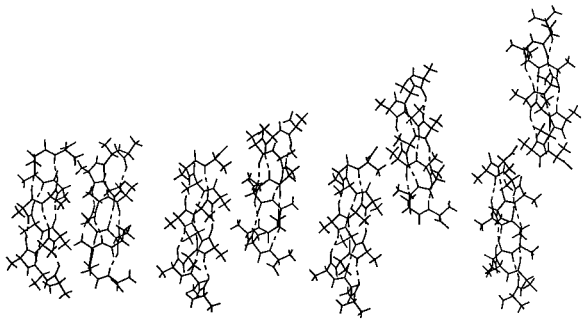

FIGURE 10 Snapshots of α-helix longitudinal shearing for two $(Ala)_{12}$ oligopeptides.

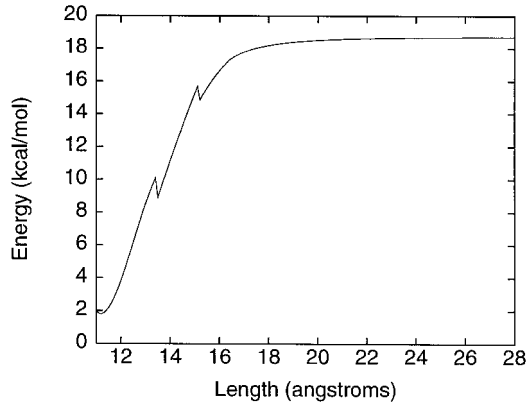

FIGURE 11 α-Helix lateral shearing: conformational energy as a function of length.

the structural elements and the nature of the energy components involved in the deformation. β-Ribbon longitudinal shearing and α-helix stretching are at the top of the list in terms of the force necessary to destroy them, followed by lateral shearing of an α-helix dimer, longitudinal shearing of the same structure, and, finally, lateral shearing of the β-ribbon. It is striking that the forces involved vary by roughly a factor of 20, whereas the corresponding deformation energies vary by only a factor of 2. In fact, it can be seen that the deformation energy has little correlation with the forces involved. This is clear both in the case of the β-ribbon and of the α-helix dimer, for which very different forces are found for longitudinal and lateral shearing, although the total deformation energy in each case is necessarily identical. It can also be noted that whether the forces depend on the length of the structural element or not is a subtle function of the type of deformation and of the dominant energy component. Thus, only longitudinal shearing of the β-ribbon shows a length dependence, whereas only lateral shearing has a length dependence for the α-helix dimer.

All of these differences can be understood by looking at the nature of the dominant energy component that resists the destruction of the structural element in question. α-Helices are difficult to stretch principally because of torsional potentials which resist unwinding of the polypeptide backbone along a vector parallel to the helical axis. Even though the helix is likely to unravel turn by turn (leading to little length dependence), it can be noted that these forces are considerably greater than the peak force necessary to break a single hydrogen bond with our modeling approach ($\sim$ 150 pN). Longitudinal shearing of β-ribbons is dominated by the coupled strength of the hydrogen bonds that lie perpendicular to the ribbon axis. The total force necessary is thus roughly the corresponding multiple of the force necessary to break a single bond (again, $\sim$150 pN, although the movement is now perpendicular to rather than along the hydrogen bond axis). This leads to a considerable resistance and a strong length dependence. In contrast, lateral shearing of the β-ribbon requires only one hydrogen bond to be broken at a time, which leads to very low average forces ($\sim$40 pN) and no length dependence. (It can be remarked that even the peak forces in this case are below the hydrogen bond breaking threshold because of a compensating effect due to released torsional strain.) Lastly, longitudinal shearing of the α-helix dimer is dominated by local van der Waals contacts between the side chains and requires relatively low forces and shows little length dependence, whereas lateral shearing must break the van der Waals interactions of the entire contact surface, leading to high forces and strong length dependence.

CONCLUSIONS

We conclude that unzipping β-strands from the edges of β-sheets or longitudinally shearing apart α-helices are the most likely starting points for unraveling a globular protein. The experimental results obtained on titin, which contains β-type immunoglobulin and related fibronectin III domains, can be considered as consistent with these results. Although no intermediate steps can be seen in the denaturation process during experimental stretching of the titin fiber, the measured forces, which range from 20 to 250 pN, are coherent with our modeling of the lateral shearing of β-domains (although any quantitative comparison is made difficult by the range of the experimental results and the fact that they are dependent on the loading rate) (Evans and Ritchie, 1997). It is interesting to add that a recent MD simulation of titin stretching (Lu et al., 1998) led to longitudinal β shearing with rupture forces $\sim$2 pN. In this case, our results would predict a rotation of the protein domain to allow lateral shearing.

On the basis of our results it is also possible to predict that mixed α/β or pure α proteins will be more difficult to completely denature by pulling and that one might reasonably expect to be able to distinguish the separation of helices from the destruction of their internal structure. The latter step appears to involve forces that are well beyond those seen for titin or, for that matter, measured in single-molecule stretching experiments on DNA (Cluzel et al., 1996; Smith et al., 1996) (although one must again be

TABLE 1 Summary of the structural deformations studied

Structure	Dominant energy component	ΔEnergy (kcal/mol)	Force (pN)	Length dependence
α stretch	Torsion	~50	~500	No
β longitudinal shear	H bond	~40	~1000	Yes
β lateral shear	H bond	~40	~40–120	No
α_2 longitudinal shear	van der Waals	~20	~65–150	No
α_2 lateral shear	van der Waals	~20	~200	Yes

Approximate deformation energies and forces are given for secondary structural elements of the lengths typically found in globular proteins.

prudent in noting that certain α-helices may be disrupted simply by being isolated from their protein environment).

It is clear that we have treated only idealized cases in this modeling study and that we are using a very simple environmental representation. Although we have adjusted hydrogen bonding to correspond to aqueous solution values, it is not easy to guess how solvent molecules will change the van der Waals component of interactions as the protein structure comes apart. In addition, the structural elements we have treated in isolation will generally appear in other interactions within a globular protein (helix bundles, helix-sheet packing, β-barrels, etc.), which will complicate their behavior. Finally, we have presently ignored sequence effects, studying only oligoalanine peptides. (Sequence effects might be expected to play a major role principally for α-helix separations.)

The biological relevance of this modeling and, particularly, its possible relationship to protein unfolding is presently difficult to judge. Our results on isolated or paired secondary structural elements suggest that protein force spectra may generally be richer than those seen in the case of titin. However, if folding intermediates are indeed rare, at least for small, rapidly folding proteins (Fersht, 1995; Mirny et al., 1996) this may not turn out to be the case. It should also be stressed that mechanically induced denaturation imposes an unnatural unfolding pathway, although it does have the advantage that the native structure is destroyed under normal physiological conditions. Although this approach seems poorly adapted to locating folding intermediates, it may be able to differentiate states of very different compactness, such as the unfolding of a single domain within a multi-domain protein. It may also serve to better characterize the structural building blocks that form early on the folding pathway and also to investigate the influence of point mutations on their stability (Shortle, 1996).

We acknowledge funding under the IFCPAR contract 1804–1, and R. Rohs thanks the Deutscher Akademischer Austauschdienst for funding his research stay in the Laboratoire de Biochimie Théorique.

REFERENCES

Ahora, N., and B. Jayaram. 1997. Strength of hydrogen bonds in α-helices. *J. Comp. Chem.* 18:1245–1252.

Allemand, J. F., D. Bensimon, R. Lavery, and V. Croquette. 1998. Stretched and overwound DNA forms a Pauling-like structure with exposed bases. *Proc. Natl. Acad. Sci. U.S.A.* 95:14152–14157.

Austin, R. H., J. P. Brody, E. C. Cox, T. Duke, and W. Volkmuth. 1997. Stretch genes. *Physics Today*. 50:32–38.

Bensimon, D. 1996. Force: a new structural control parameter? *Curr. Biol.* 4:885–889.

Bockelmann, U., B. Essevaz-Roulet, and F. Heslot. 1997. Molecular stick-slip motion revealed by opening DNA with piconewton forces. *Phys. Rev. Lett.* 79:4489–4492.

Cluzel, P., A. Lebrun, C. Heller, R. Lavery, J. L. Viovy, D. Chatenay, and F. Caron. 1996. DNA: an extensible molecule. *Science*. 271:792–794.

Essevaz-Roulet, B., U. Bockelmann, and F. Heslot. 1997. Mechanical separation of complementary strands of DNA. *Proc. Natl. Acad. Sci. U.S.A.* 94:11935–11940.

Evans, E., and K. Ritchie. 1997. Dynamic strength of molecular adhesion bonds. *Biophys. J.* 72:1541–1555.

Fersht, A. R. 1995. Optimization of rates of protein folding: the nucleation-condensation mechanism and its implications. *Proc. Natl. Acad. Sci. U.S.A.* 92:10869–10873.

Florin, E.-L., V. T. Moy, and H. E. Gaub. 1994. Adhesion forces between individual ligand-receptor pairs. *Science*. 264:415–417.

Grubmüller, H., B. Heynmann, and P. Tavan. 1996. Ligand binding: molecular mechanics calculation of the streptavidin-biotin rupture force. *Science*. 271:997–999.

Hingerty, B., R. H. Richie, T. L. Ferrel, and J. E. Turner. 1985. Dielectric effects in biopolymers: the theory of ionic saturation revisited. *Biopolymers*. 24:427–439.

Izrailev, S., S. Stepaniants, M. Balsera, Y. Oono, and K. Schulten. 1997. Molecular dynamics study of unbinding of the avidin-biotin complex. *Biophys. J.* 72:1568–1581.

Kellermayer, M. S. Z., S. B. Smith, H. L. Granzier, and C. Bustamante. 1997. Folding-unfolding transitions in single titin molecules characterized with laser tweezers. *Science*. 276:1112–1116.

Konrad, M. W., and J. L. Bolonick. 1996. Molecular dynamics simulation of DNA stretching is consistent with the tension observed for extension and strand separation and predicts novel ladder structure. *J. Am. Chem. Soc.* 118:10989–10994.

Lavery, R., I. Parker, and J. Kendrick. 1986. A general approach to the optimization of the conformation of ring molecules with an application to valinomycin. *J. Biomol. Struct. Dyn.* 4:443–462.

Lavery, R., K. Zakrzewska, and H. Sklenar. 1995. JUMNA (JUnction Minimisation of Nucleic Acids). *Comp. Phys. Commun.* 91:135–158.

Lebrun, A., and R. Lavery. 1996. Modeling extreme stretching of DNA. *Nucleic Acids Res.* 24:2260–2270.

Lebrun, A., and R. Lavery. 1998. Modeling the mechanics of a DNA oligomer *J. Biomol. Struct. Dyn.* 16:593–604.

Lebrun, A., Z. Shakked, and R. Lavery. 1997. Local DNA stretching mimics the distorsion caused by the TATA box-binding protein. *Proc. Natl. Acad. Sci. U.S.A.* 94:2993–2998

Lee, G. U., L. A. Chrisey, and R. A. Colton. 1994a. Direct measurement of the forces between complementary strands of DNA. *Science*. 266: 771–776.

Lee, G. U., D. A. Kidwell, and R. C. Colton. 1994b. Sensing discrete streptavidin-biotin interactions with atomic force microscopy. *Langmuir*. 10:354–357.

Lu, H., B. Isralewitz, A. Krammer, V. Vogel, and K. Schulten. 1998. Unfolding of titin immunoglobin domains by steered molecular dynamics simulation. *Biophys. J.* 75:662–671.

Mirny, L. A., V. Abkevich, and E. I. Shakhnovich. 1996. Universality and diversity of the protein folding scenarios: a comprehensive analysis with the aid of a lattice model. *Curr. Biol.* 1:103–116.

Noy, A., D. V. Vezenov, J. F. Kayyem, T. J. Meade, and C. M. Lieber. 1997. Stretching and breaking duplex DNA by chemical force microscopy. *Chem. Biol.* 4:519–527.

Press, W. H., S. A. Teukolsky, W. T. Vettering, and B. P. Flannery (editors). 1992. Numerical recipes in Fortran. Cambridge University Press, Cambridge, UK.

Rief, M., M. Gautel, F. Oesterhelt, J. O. Fernandez, and H. E. Gaub. 1997a. Reversible unfolding of individual titin immunoglobulin domains by AFM. *Science*. 276:1109–1112.

Rief, M., F. Oesterhelt, B. Heymann, and H. E. Gaub. 1997b. Single molecule force spectroscopy on polysaccharides by atomic force microscopy. *Science*. 275:1295–1297.

Shortle, D. 1996. The denatured state (the other half of the folding equation) and its role in protein stability. *FASEB J.* 10:27–34.

Smith, S. B., Y. Cui, and C. Bustamante. 1996. Overstretching B-DNA: the elastic response of individual double-stranded and single-stranded DNA molecules. *Science*. 271:795–799.

Strick, T. R., J. F. Allemand, D. Bensimon, A. Bensimon, and V. Croquette. 1996. The elasticity of a single supercoiled DNA molecule. *Science*. 271:1835–1837.

Strick, T. R., J. F. Allemand, D. Bensimon, and V. Croquette. 1998. Behavior of supercoiled DNA. *Biophys. J.* 74:2016–2028.

Tskhovrebova, L., J. Trinick, J. A. Sleep, and R. M. Simmons. 1997. Elasticity and unfolding of single molecules of the giant muscle protein titin. *Nature*. 387:308–312.

Yin, H., M. D. Wang, K. Svoboda, R. Landick, S. M. Block, and J. Gelles. 1995. Transcription against an applied force. *Science*. 270:1653–1657.

Zakrzewska, K., and A. Pullman. 1985. Optimized monopoles expansions for the representation of the electrostatic properties of polypeptides and proteins. *J. Comp. Chem.* 6:265–273.